

MDPI

Article

Fusion of Bilateral 2DPCA Information for Image Reconstruction and Recognition

Jing Wang ^{1,2,*}, Mengli Zhao ^{1,2}, Xiao Xie ^{1,2}, Li Zhang ^{1,2,3,*} and Wenbo Zhu ⁴

- School of Computer and Information Technology, Xinyang Normal University, Xinyang 464000, China
- Henan Key Laboratory of Analysis and Applications of Education Big Data, Xinyang Normal University, Xinyang 464000, China
- School of Computer and Artificial Intelligence, Zhengzhou University, Zhengzhou 450000, China
- School of Mechatronic Engineering and Automation, Foshan University, Foshan 525000, China
- * Correspondence: wangjing@xynu.edu.cn (J.W.); zhangli@xynu.edu.cn (L.Z.)

Abstract: Being an efficient image reconstruction and recognition algorithm, two-dimensional PCA (2DPCA) has an obvious disadvantage in that it treats the rows and columns of images unequally. To exploit the other lateral information of images, alternative 2DPCA (A2DPCA) and a series of bilateral 2DPCA algorithms have been proposed. This paper proposes a new algorithm named direct bilateral 2DPCA (DB2DPCA) by fusing bilateral information from images directly—that is, we concatenate the projection results of 2DPCA and A2DPCA together as the projection result of DB2DPCA and we average between the reconstruction results of 2DPCA and A2DPCA as the reconstruction result of DB2DPCA. The relationships between DB2DPCA and related algorithms are discussed under some extreme conditions when images are reshaped. To test the proposed algorithm, we conduct experiments of image reconstruction and recognition on two face databases, a handwritten character database and a palmprint database. The performances of different algorithms are evaluated by reconstruction errors and classification accuracies. Experimental results show that DB2DPCA generally outperforms competing algorithms both in image reconstruction and recognition. Additional experiments on reordered and reshaped databases further demonstrate the superiority of the proposed algorithm. In conclusion, DB2DPCA is a rather simple but highly effective algorithm for image reconstruction and recognition.

Keywords: DB2DPCA; bilateral 2DPCA; image reconstruction; image recognition; face recognition



Citation: Wang, J.; Zhao, M.; Xie, X.; Zhang, L.; Zhu, W. Fusion of Bilateral 2DPCA Information for Image Reconstruction and Recognition. Appl. Sci. 2022, 12, 12913. https://doi.org/10.3390/app122412913

Academic Editor: João M. F. Rodrigues

Received: 19 November 2022 Accepted: 14 December 2022 Published: 15 December 2022

Publisher's Note: MDPI stays neutral with regard to jurisdictional claims in published maps and institutional affiliations.



Copyright: © 2022 by the authors. Licensee MDPI, Basel, Switzerland. This article is an open access article distributed under the terms and conditions of the Creative Commons Attribution (CC BY) license (https://creativecommons.org/licenses/by/4.0/).

1. Introduction

In the field of machine learning and pattern recognition, feature extraction from massive high-dimensional data is a very demanding job [1]. Various applications of feature extraction methods include face recognition [2], EEG-based emotion recognition [3], rice disease recognition [4], facial emotion recognition [5], speaker recognition [6] and diagnosis of COVID-19 related diseases [7,8].

One of the most prevalent feature extraction methods is Principal Component Analysis (PCA) [9,10], which seeks a projection matrix that maximizes projected variance. PCA is a simple, non-parametric technique for extracting relevant information from large datasets, minimizing information loss, reducing the dimensionality of such datasets and increasing interpretability. It is abundantly applied in different disciplines including atmospheric science [10], computer science [11] and neuroscience [12].

When applying PCA to extract features from images, 2D image matrices should be reshaped into 1D image vectors prior [11]. This operation abandons the 2D image spatial structure information and leads to a large size of covariance matrix that is difficult to handle. Two-dimensional PCA (2DPCA) [13] alleviates this problem by dealing with image matrices directly rather than reshaping them into vectors. Compared with PCA, 2DPCA extracts more structural information from images and its covariance matrix becomes much easier

to handle. Moreover, 2DPCA generally outperforms PCA in image reconstruction and recognition [13]. Due to its simple formulation and superior performance, 2DPCA has been successfully applied in various fields such as image retrieval [14,15], fault detection [16], iris recognition [17], target recognition based on synthetic aperture radar images [18], bearing fault diagnosis [19], brain tumor diagnosis [20], etc.

Despite having many advantages, 2DPCA treats the rows and columns of images unequally, thus lacking symmetry in its theory. Specifically, to extract features from an image by 2DPCA, rows rather than columns of the image are projected onto the principal components. In order to project the other direction, i.e., columns of the image, the alternative 2DPCA (A2DPCA) [21] was proposed. Then, it is natural to combine the two kinds of unilateral 2DPCA. Following this idea, $(2D)^2$ PCA [21], generalized 2DPCA (G2DPCA) [22] and sequential row–column 2DPCA (RC2DPCA) [23] were proposed in order to fuse the bilateral information of images. $(2D)^2$ PCA calculates bilateral eigenvectors by directly taking the projection matrices from 2DPCA and A2DPCA. Generalized 2DPCA calculates bilateral eigenvectors by iteratively solving a minimization problem. RC2DPCA calculates bilateral eigenvectors in two stages, i.e., first performing 2DPCA in the row direction on the original data and then performing A2DPCA in the column direction on the projected results of the first stage. All of these algorithms project an image onto the two lateral eigenvectors simultaneously in order to compute the final projection results.

In this paper, we propose a novel bilateral 2DPCA by fusing 2DPCA and A2DPCA in a direct fashion, called Direct Bilateral 2DPCA (DB2DPCA). Unlike the previously proposed bilateral 2DPCA algorithms, we concatenate the projection results of 2DPCA and A2DPCA together for projection, and we take the average reconstruction results of 2DPCA and A2DPCA for reconstruction. The proposed method has three advantages. First, it has a symmetric property in the sense that it treats the rows and columns of images equally. Second, for projection, it concatenates the bilateral information rather than mixing them together. Therefore, it extracts more features than lateral algorithms or other previously proposed bilateral algorithms. For reconstruction, it simply averages two lateral results, thus being more interpretable than other bilateral algorithms. Third, it is rooted in 2DPCA and A2DPCA; so, the computational time to extract features by DB2DPCA will be no longer than those of other bilateral algorithms.

The contributions of our work are summarized in the following points:

- 1. A novel, bilateral 2DPCA—i.e., DB2DPCA—is proposed by fusing two unilateral 2DPCA algorithms. We concatenate the projection results of 2DPCA and A2DPCA together for projection and take the average reconstruction results of 2DPCA and A2DPCA for reconstruction. By this way, we can extract more features from images and obtain a more interpretable reconstruction model.
- We evaluate DB2DPCA in the tasks of image recognition and reconstruction on four widely used benchmark databases. The experimental results demonstrate that the proposed algorithm outperforms competing algorithms.
- Additional experiments on reordered and reshaped images further demonstrate the superiority of DB2DPCA in image recognition.

The remainder of this paper is organized as follows. Section 2 reviews the recent advances of 2DPCA. Section 3 describes the competing algorithms and the proposed DB2DPCA algorithm. Section 4 conducts experiments of image reconstruction and classification to evaluate the performance of DB2DPCA. Section 5 shows the experimental results. Section 6 provides discussions on this study and related works. Finally, Section 7 presents the conclusions.

2. Related Works

Besides the unilateral and bilateral 2DPCA-based algorithms mentioned above, there are many other advances of 2DPCA, as discussed below.

To extract more structure information from images, Titijaroonroj et al. [24] and Sahoo et al. [25,26] made improvements on the traditional 2DPCA by utilizing it on subimages

Appl. Sci. 2022, 12, 12913 3 of 25

of the original image. The subimages are generated by sliding a window on the original image or by partitioning the original image into blocks. By this way, they can extract more structure information from images. However, the procedures of these algorithms are complex and their performances are largely determined by how the image is partitioned.

Traditional 2DPCA utilizes ℓ_2 -norm as the distance metric, which aggravates the effect of outliers on the objective function. On the other hand, the features extracted by 2DPCA are dense, which means that 2DPCA cannot automatically eliminate irrelevant features. To introduce robustness and sparsity into traditional 2DPCA, several algorithms have been proposed. Li et al. [27] and Wang et al. [28] replaced ℓ_2 -norm with ℓ_1 -norm on the objective function of 2DPCA to improve its robustness, and proposed the greedy 2DPCA-L1 and the non-greedy 2DPCA-L1. Yang et al. [29] further replaced ℓ_1 -norm with transformed ℓ_1 -norm, which is expected to be more robust, and proposed the 2DPCA- $T\ell_1$. Wang and Wang [30] imposed ℓ_1 -norm both on the objective function and the constraint of 2DPCA for simultaneously robust and sparse modeling, and proposed the 2DPCAL1-S. Considering that replacing ℓ_2 -norm with ℓ_1 -norm brings many benefits to the related algorithms, it is worthwhile to replace the two norms by an arbitrary norm, i.e., ℓ_p -norm, to exploit more possibilities. Based on this idea, Wang [31] imposed ℓ_p -norm both on the objective function and the constraint of 2DPCA, and proposed the generalized 2DPCA with ℓ_p -norm (G2DPCA-Lp), further enhancing its robustness and sparseness.

Rotational invariance is another desired property of 2DPCA-based algorithm which can be introduced by $\ell_{2,1}$ -norm or F-norm. $\ell_{2,1}$ -norm is a rotational invariant ℓ_{1} -norm, hence the name R_1 -norm [32,33]. Gao et al. [34] introduced R_1 -norm into 2DPCA and proposed the R_1 -2DPCA. Li et al. [35] replaced square F-norm with F-norm in 2DPCA and proposed the F-2DPCA. Gao et al. [36] minimized the ratio of reconstruction error to the projected variances that are measured with *F*-norm, and proposed the Angle-2DPCA. Wang and Li [37] minimized the product of reconstruction error and projected variance that are measured with F-norm and proposed the Area-2DPCA. Wang et al. [38] maximized the ratio of projected variance to original data that are measured with F-norm and proposed the Cos-2DPCA. Bi et al. [39] maximized the ratio of projected variance to original data that are measured with R_1 -norm and considered the optimal mean in data centralization, proposing the robust optimal mean cosine angle 2DPCA (ROMCA-2DPCA). Razzak et al. [40] introduced 2D outliers-robust PCA (ORPCA) by relaxing the orthogonal constraints and penalizing the regression coefficient. Inspired by extending ℓ_2 -norm and ℓ_1 -norm to ℓ_p -norm, the $\ell_{2,1}$ -norm and F-norm were extended to arbitrary powers correspondingly. By extending $\ell_{2,1}$ -norm to $\ell_{2,p}$ -norm, Mi et al. [41] proposed the $\ell_{2,p}$ -2DPCA, Zhou et al. [42] proposed the generalized centered 2DPCA (GC-2DPCA). By extending F-norm to F_p -norm, Kuang et al. [43] proposed the F_p -2DPCA. Following the two-stage idea of RC2DPCA [23], Zhou et al. [44] proposed the bilateral Angle-2DPCA (BA2DPCA), Bi et al. [45] proposed the $\ell_{2,p}$ -norm sequential bilateral 2DPCA ($\ell_{2,p}$ -SB-2DPCA).

To directly address the three color channels of an image, color 2DPCA-based algorithms were proposed. Xiang et al. [46] used a row vector to represent the color channel and proposed the color-2DPCA (C-2DPCA). Jia et al. [47] used a quaternion with zero real part to represent the color channel and proposed the 2D quaternion PCA (2D-QPCA). Xiao and Zhou [48] proposed a novel quaternion ridge regression model for 2D-QPCA and proposed the QRR-2D-QPCA. Wang et al. [49] replaced square F-norm with F-norm in 2D-QPCA and proposed the F-2D-QPCA. Jia et al. [50] replaced ℓ_2 -norm with ℓ_p -norm in 2D-QPCA and proposed the generalized 2D-QPCA (G-2D-QPCA). Zhao et al. [51] introduced ℓ_p -norm to 2D-QPCA and proposed the relaxed 2DPCA (R-2DPCA).

Besides those mentioned above, Zhang et al. [52] replaced the *F*-norm with nuclear-norm in traditional 2DPCA and generalized 2DPCA [22], proposing the nuclear-norm-based 2DPCA (N-2DPCA) and the nuclear-norm-based bilateral 2DPCA (NB-2DPCA). Zhang et al. [53] proposed a computationally efficient Riemannian proximal stochastic gradient descent algorithm (RPSGD) to solve sparse 2DPCA on the Stiefel manifold. Li et al. [54] introduced the human learning mechanism to 2DPCA and proposed the self-paced 2DPCA

Appl. Sci. 2022, 12, 12913 4 of 25

(SP2DPCA). Wang et al. [55] applied the Lanczos algorithm to speed up traditional 2DPCA. Further, 2DPCA was employed to design novel neural networks such as 2DPCA-Net [56] and L1-2DPCA-Net [57].

In summary, recent advances of 2DPCA mainly focus on partitioning images into subregions to extract more structural information, introducing robustness and sparsity by ℓ_1 -norm or ℓ_p -norm, introducing rotational invariance by $\ell_{2,1}$ -norm or F-norm, processing color images directly under the quaternion framework, designing deep learning models, etc., as shown in Table 1. Note that some algorithms in this table incorporate multiple ideas but we still classify each of them into a single category for simplicity. For example, $\ell_{2,p}$ -SB-2DPCA [45] incorporates the arbitrary power of $\ell_{2,1}$ -norm and the sequential bilateral idea from RC2DPCA [23].

Table 1. Recent advances of 2DPCA.

Category	Bibliography	Algorithm
Bilateral algorithms	Zhang et al. [21]	$(2D)^2$ PCA
<u> </u>	Kong et al. [22]	Generalized 2DPCA
	Yang et al. [23]	RC2DPCA
Subimages	Titijaroonroj et al. [24]	RCM-2DPCA
	Sahoo et al. [25]	ESIMPCA, EFLPCA
	Sahoo et al. [26]	Bi-ESIMPCA, Bi-EFLPCA
Robust and sparse modelling	Li et al. [27]	2DPCA-L1
1	Wang et al. [28]	non-greedy 2DPCA-L1
	Yang et al. [29]	2DPCA- $T\ell_1$
	Wang and Wang [30]	2DPCAL1-S
	Wang [31]	G2DPCA
Rotational invariance	Gao et al. [34]	R_1 -2DPCA
	Li et al. [35]	F-2DPCA
	Gao et al. [36]	Angle-2DPCA
	Wang and Li [37]	Area-2DPCA
	Wang et al. [38]	Cos-2DPCA
	Bi et al. [39]	ROMCA-2DPCA
	Razzak et al. [40]	ORPCA
	Mi et al. [41]	$\ell_{2,p}$ -2DPCA
	Zhou et al. [42]	GC-2DPCA
	Kuang et al. [43]	F_p -2DPCA
	Zhou et al. [44]	BA2DPCA
	Bi et al. [45]	$\ell_{2,p}$ -SB-2DPCA
Color image processing	Xiang et al. [46]	C-2DPCA
	Jia et al. [47]	2D-QPCA
	Xiao and Zhou [48]	QRR-2D-QPCA
	Wang et al. [49]	F-2D-QPCA
	Jia et al. [50]	G-2D-QPCA
	Zhao et al. [51]	R-2DPCA
Nuclear norm	Zhang et al. [52]	N-2DPCA, NB-2DPCA
Stiefel manifold	Zhang et al. [53]	RPSGD-S2DPCA
Human learning mechanism	Li et al. [54]	SP2DPCA
Lanczos algorithm	Wang et al. [55]	Lanczos-2DPCA
Deep learning model	Yu and Wu [56]	2DPCA-Net
	Li et al. [57]	L1-2DPCA-Net

3. Methodology

Few of the algorithms in Table 1 pay attention to fusing bilateral information of images, which is the focus of this paper. In the following paper, lowercase letters denote scalars, boldface lowercase letters denote vectors and boldface uppercase letters denote matrices. We first review related algorithms, i.e., PCA, 2DPCA, A2DPCA and (2D)²PCA, in order. Then, the proposed DB2DPCA algorithm is described and its relationships with the four related algorithms are discussed.

Appl. Sci. **2022**, 12, 12913 5 of 25

3.1. PCA

Suppose there are n training image samples $\mathbf{X}_1, \mathbf{X}_2, ..., \mathbf{X}_n$, where $\mathbf{X}_i \in \mathbb{R}^{h \times w}$; i = 1, 2, ..., n; and h and w are the image height and image width, respectively. Let $d = h \times w$. When applying PCA for image analysis, 2D image matrices should be reshaped into corresponding 1D image vectors prior [11], generating $\mathbf{y}_1, \mathbf{y}_2, ..., \mathbf{y}_n$, where $\mathbf{y}_i \in \mathbb{R}^{d \times 1}$, i = 1, 2, ..., n. PCA [9,10] aims at finding a projection matrix $\mathbf{W} \in \mathbb{R}^{d \times m}$ by maximizing the total scatter of projected image samples as follows:

$$\max_{\mathbf{W}^T \mathbf{W} = \mathbf{I}_m} tr \mathbf{W}^T \frac{1}{n-1} \sum_{i=1}^n (\mathbf{y}_i - \overline{\mathbf{y}}) (\mathbf{y}_i - \overline{\mathbf{y}})^T \mathbf{W}, \tag{1}$$

where m is the feature number, $\mathbf{I}_m \in \mathbb{R}^{m \times m}$ denotes an identity matrix, $tr(\cdot)$ denotes the trace of a matrix and $\overline{\mathbf{y}} = \frac{1}{n} \sum_{i=1}^{n} \mathbf{y}_i$ denotes the mean image vector. By eigenvalue decomposition of the covariance matrix [9,10]

$$\mathbf{S} = \frac{1}{n-1} \sum_{i=1}^{n} (\mathbf{y}_i - \overline{\mathbf{y}}) (\mathbf{y}_i - \overline{\mathbf{y}})^T \in \mathbb{R}^{d \times d}, \tag{2}$$

we can obtain m eigenvalues $\lambda_1, \lambda_2, ..., \lambda_m$ and corresponding eigenvectors $\mathbf{w}_1, \mathbf{w}_2, ..., \mathbf{w}_m$. Without loss of generality, we assume that the eigenvalues are sorted in descending order. The eigenvectors are the principal components and they make up the projection matrix \mathbf{W} . The percentage of total variance [10] explained by these principal components is

$$\frac{\sum_{i=1}^{m} \lambda_i}{\sum_{i=1}^{n} \lambda_i}.$$
 (3)

For a test image sample $\widetilde{\mathbf{y}} \in \mathbb{R}^{d \times 1}$, its feature matrix is

$$(\widetilde{\mathbf{y}} - \overline{\mathbf{y}})^T \mathbf{W} \in \mathbb{R}^{1 \times m}. \tag{4}$$

The reconstruction result of sample $\tilde{\mathbf{y}}$ is

$$\mathbf{W}\mathbf{W}^{T}(\widetilde{\mathbf{y}} - \overline{\mathbf{y}}) + \overline{\mathbf{y}} \in \mathbb{R}^{d \times 1}.$$
 (5)

It can be further reshaped from a vector into a $h \times w$ image matrix in order to generate the reconstruction image. Eigenvalue decomposition of the covariance matrix \mathbf{S} is difficult since the size of \mathbf{S} is huge.

3.2. 2DPCA

In contrast to traditional PCA, 2DPCA [13] depends on 2D image matrices rather than 1D image vectors. Therefore, the image matrices do not need to be reshaped into vectors prior. Instead, an image covariance matrix can be constructed based on the image matrices in a direct manner. To be specific, 2DPCA [13] aims at finding a projection matrix $\mathbf{U} \in \mathbb{R}^{w \times k}$

$$\max_{\mathbf{U}^T\mathbf{U}=\mathbf{I}_k} tr \mathbf{U}^T \frac{1}{n-1} \sum_{i=1}^n (\mathbf{X}_i - \overline{\mathbf{X}})^T (\mathbf{X}_i - \overline{\mathbf{X}}) \mathbf{U},$$
 (6)

where k is the feature number and $\overline{\mathbf{X}} = \frac{1}{n} \sum_{i=1}^{n} \mathbf{X}_{i}$ denotes the mean image. The projection matrix \mathbf{U} is calculated by eigen-decomposition of the image covariance matrix

$$\frac{1}{n-1} \sum_{i=1}^{n} (\mathbf{X}_i - \overline{\mathbf{X}})^T (\mathbf{X}_i - \overline{\mathbf{X}}) \in \mathbb{R}^{w \times w}$$
 (7)

Appl. Sci. **2022**, 12, 12913 6 of 25

and then selecting the eigenvectors corresponding to the k largest eigenvalues [13]. The percentage of total variance explained by these eigenvectors can be calculated similar to Equation (3). For a test image sample $\tilde{\mathbf{X}} \in \mathbb{R}^{h \times w}$, its feature matrix is

$$(\widetilde{\mathbf{X}} - \overline{\mathbf{X}})\mathbf{U} \in \mathbb{R}^{h \times k}.$$
 (8)

The reconstruction image of sample $\widetilde{\mathbf{X}}$ is

$$(\widetilde{\mathbf{X}} - \overline{\mathbf{X}})\mathbf{U}\mathbf{U}^T + \overline{\mathbf{X}} \in \mathbb{R}^{h \times w}. \tag{9}$$

The original 2DPCA only projects the rows of images onto the projection matrix, as shown in Equations (6) and (8). Therefore, 2DPCA lacks symmetry in the sense that it treats the rows and columns of images unequally.

3.3. Alternative 2DPCA

Since 2DPCA only deals with one direction of images, it is necessary to propose an algorithm to deal with the other direction of images. This idea leads to A2DPCA [21]. A2DPCA aims to find a projection matrix $\mathbf{V} \in \mathbb{R}^{h \times l}$ by solving the following optimization problem:

$$\max_{\mathbf{V}^T \mathbf{V} = \mathbf{I}_l} tr \mathbf{V}^T \frac{1}{n-1} \sum_{i=1}^n (\mathbf{X}_i - \overline{\mathbf{X}}) (\mathbf{X}_i - \overline{\mathbf{X}})^T \mathbf{V},$$
(10)

where l is the feature number. Similarly, \mathbf{V} could be calculated by eigen-decomposition of the image covariance matrix

$$\frac{1}{n-1} \sum_{i=1}^{n} (\mathbf{X}_i - \overline{\mathbf{X}}) (\mathbf{X}_i - \overline{\mathbf{X}})^T \in \mathbb{R}^{h \times h}$$
(11)

and then selecting the eigenvectors corresponding to the l largest eigenvalues [21]. The percentage of total variance explained by these eigenvectors can be calculated likewise. For a test image sample $\widetilde{\mathbf{X}}$, its feature matrix is

$$\mathbf{V}^T(\widetilde{\mathbf{X}} - \overline{\mathbf{X}}) \in \mathbb{R}^{l \times w}. \tag{12}$$

The reconstruction image of sample \tilde{X} is

$$\mathbf{V}\mathbf{V}^{T}(\widetilde{\mathbf{X}} - \overline{\mathbf{X}}) + \overline{\mathbf{X}} \in \mathbb{R}^{h \times w}.$$
(13)

A2DPCA only projects the columns of images onto the projection matrix. It also lacks symmetry, the same as 2DPCA.

3.4. $(2D)^2 PCA$

 $(2D)^2$ PCA [21], G2DPCA [22] and RC2DPCA [23] are three representatives of existing bilateral 2DPCA algorithms. All of them project an image onto the two lateral eigenvectors simultaneously in order to calculate the feature matrix. Their only difference lies in the way to calculate bilateral eigenvectors. Since $(2D)^2$ PCA shares the same eigenvectors with the two unilateral 2D algorithms but the eigenvectors of G2DPCA and RC2DPCA are quite different, we focus on $(2D)^2$ PCA in our paper. By this way, we can make a fair comparison between this bilateral 2D algorithm and the two unilateral 2D algorithms.

To make the most of bilateral information, $(2D)^2PCA$ [21] directly takes the projection matrices **U** and **V** from 2DPCA and A2DPCA, respectively. For a test image sample $\widetilde{\mathbf{X}}$, its feature matrix projected by $(2D)^2PCA$ is

$$\mathbf{V}^T(\widetilde{\mathbf{X}} - \overline{\mathbf{X}})\mathbf{U} \in \mathbb{R}^{l \times k}. \tag{14}$$

Appl. Sci. **2022**, 12, 12913 7 of 25

The reconstruction image of sample $\widetilde{\mathbf{X}}$ reconstructed by $(2D)^2PCA$ is

$$\mathbf{V}\mathbf{V}^{T}(\widetilde{\mathbf{X}} - \overline{\mathbf{X}})\mathbf{U}\mathbf{U}^{T} + \overline{\mathbf{X}} \in \mathbb{R}^{h \times w}.$$
 (15)

(2D)²PCA overcomes the limitations of the two unilateral 2D algorithms by projecting the rows and columns of images onto two lateral eigenvectors simultaneously. Zhang and Zhou [21] demonstrated that compared with the two unilateral 2D algorithms, (2D)²PCA achieves the same classification accuracies on the Olivetti Research Laboratory (ORL) face database and achieves higher classification accuracies on a partial Face Recognition Technology (FERET) database. However, its formulation mixes bilateral information from images together and may lead to information loss. The other two unilateral algorithms, i.e., G2DPCA [22] and RC2DPCA [23], have the same problem.

3.5. Direct Bilateral 2DPCA

In this paper, we propose a novel, bilateral 2DPCA called DB2DPCA by fusing the two unilateral algorithms, i.e., 2DPCA and A2DPCA, in a direct fashion—that is, DB2DPCA takes the projection matrices **U** and **V** from the two unilateral algorithms, respectively, the same as $(2D)^2$ PCA. The difference between the two bilateral algorithms is that $(2D)^2$ PCA projects an image onto two lateral projection matrices simultaneously while DB2DPCA projects an image onto a single lateral projection matrix each time and then combines the results from two laterals together.

For a test image sample \widetilde{X} , its feature matrix by DB2DPCA is calculated by concatenating the feature matrices of 2DPCA and A2DPCA as

$$\left[vec\left((\widetilde{\mathbf{X}} - \overline{\mathbf{X}})\mathbf{U}\right); vec\left(\mathbf{V}^{T}(\widetilde{\mathbf{X}} - \overline{\mathbf{X}})\right)\right] \in \mathbb{R}^{(h \times k + l \times w) \times 1},\tag{16}$$

where $vec(\cdot)$ means to transform a matrix into a column vector by taking elements from the matrix in a column-wise manner. Figure 1 shows an illustration of this operation that transforms a matrix **A** into a column vector **b**, i.e., $\mathbf{b} = vec(\mathbf{A})$.

$$\mathbf{A} = \begin{bmatrix} a_{11} & a_{12} \\ a_{21} & a_{22} \\ a_{31} & a_{32} \end{bmatrix} \longrightarrow \mathbf{b} = \begin{bmatrix} a_{11} \\ a_{21} \\ a_{31} \\ a_{12} \\ a_{22} \\ a_{32} \end{bmatrix}$$

Figure 1. An illustration of transforming a matrix into a column vector by taking elements from the matrix in a column-wise manner.

The reconstruction image of sample \tilde{X} by DB2DPCA is

$$\frac{1}{2}\left[(\widetilde{\mathbf{X}} - \overline{\mathbf{X}})\mathbf{U}\mathbf{U}^T + \overline{\mathbf{X}}\right] + \frac{1}{2}\left[\mathbf{V}\mathbf{V}^T(\widetilde{\mathbf{X}} - \overline{\mathbf{X}}) + \overline{\mathbf{X}}\right] \in \mathbb{R}^{h \times w}.$$
 (17)

Appl. Sci. 2022, 12, 12913 8 of 25

Here, we use arithmetic mean to combine the reconstruction results of the two lateral 2DPCAs. However, geometric mean or other kinds of means can also be tried. In general, for two positive scalars *a* and *b*, the generalized mean [58] is defined as

$$\left(\frac{a^r + b^r}{2}\right)^{\frac{1}{r}},\tag{18}$$

when r is a real number. Two special cases of generalized means are the arithmetic mean when r = 1 and the geometric mean when r = 0. In this paper, we focus on r = 1, i.e., the arithmetic mean, in consideration of computational complexity and reconstruction performance.

The algorithm procedure of DB2DPCA is shown in Algorithm 1. First, we calculate projection matrices \mathbf{U} and \mathbf{V} by solving the optimization problems of 2DPCA and A2DPCA, i.e., Equations (6) and (10), respectively. Then, we calculate the feature matrix of a test image sample by Equation (16) which concatenates the feature matrices of the two unilateral 2D algorithms. The extracted features can be used to evaluate the performance of DB2DPCA in image classification. And we calculate the reconstruction image of a test image sample by Equation (17), which averages the reconstruction results of the two unilateral 2D algorithms. The obtained reconstruction image can be used to evaluate the performance of DB2DPCA in image reconstruction.

Algorithm 1: Algorithm procedure of DB2DPCA

Input: training image samples X_i , i = 1, 2, ..., n; feature numbers k and l.

Output: the feature matrix and the reconstruction image.

- 1. Calculate projection matrix **U** by solving Equation (6).
- 2. Calculate projection matrix V by solving Equation (10).
- 3. Calculate the feature matrix by Equation (16).
- 4. Calculate the reconstruction image by Equation (17).

By concatenating the feature matrices of 2DPCA and A2DPCA, DB2DPCA extracts more features that are useful for image recognition. By averaging the reconstruction results of 2DPCA and A2DPCA, DB2DPCA strengthens their common parts and weakens their differences; thus, it is expected to obtain better performance in image reconstruction.

3.6. Relationships between DB2DPCA and Other Algorithms

An image is essentially a sample containing $d(=h\times w)$ features after neglecting its 2D structure. To investigate the relationships between DB2DPCA and related algorithms, we reshape images into $p\times q(\geq d)$ matrices by the same rule. Three extreme conditions are stated below.

- (1) When p = 1 and q = d, we can obtain that **U** equals the projection matrix of conventional PCA and **V** = 1. In this case, the feature matrix for a test sample **Y** is calculated by concatenating two parts, wherein one part is the feature matrix calculated by PCA and the other part is the result of subtracting the mean image from the sample image. The reconstruction image of **Y** is calculated by averaging the reconstruction image of PCA and the sample image.
- (2) When p = h, q = w and the pixels in images are not reordered, the projection and reconstruction results of DB2DPCA are just integrating the results of 2DPCA and A2DPCA, as shown in Equations (16) and (17), respectively.
- (3) When p = d and q = 1, we can obtain that U = 1, and V equals the projection matrix of conventional PCA. In this case, the projection and reconstruction results of DB2DPCA are the same as the results in case of p = 1 and q = d. This shows the symmetry property of DB2DPCA.

In general, p could be an arbitrary integer satisfying $1 \le p \le d$. Thus, $q = \lfloor d/p \rfloor$ —namely, q—is the smallest integer no less than d/p. The symmetry of DB2DPCA indicates that DB2DPCA on images of size $p \times q$ approximates DB2DPCA on images of size $q \times p$.

By taking this symmetric property into consideration, we only need to change p in the range of $[1, \sqrt{d}]$ in order to investigate its effect on the performance of DB2DPCA.

Since $p \times q \ge d$, there may exist blank pixels that should be filled in a reshaped image. Some potential choices are randomly picking some pixels from the original image to fill the blanks, calculating the mean value of all pixels in the original image to fill the blanks and filling the blanks with the nearest non-blank pixels. If only the cases when d is divisible by p are considered, we can avoid the noises introduced by these operations.

4. Experiments

In order to evaluate DB2DPCA, we compare its performances in image reconstruction and recognition with four related algorithms, i.e., PCA, 2DPCA, A2DPCA and (2D)²PCA, on four image databases. To further exploit the properties of DB2DPCA, we additionally conduct image recognition experiments when the pixels in images are reordered by certain rules and when images are reshaped to different sizes.

4.1. Databases

Here, we briefly introduce the four databases used in the experiments. These are the Extended Yale B face database [59], AR face database [60], Binary Alphadigits database and PolyU 3D palmprint database [61]. These databases are used to address different kinds of recognition problems, i.e., face recognition in various lighting conditions, face recognition with occlusions, handwritten digits and letters classification, and palmprint recognition. In this way, we could make a thorough comparison between the proposed DB2DPCA and related algorithms.

The Extended Yale B face database includes 2414 cropped face images from 38 individuals, with about 64 images per individual. There exist 18 broken images in this database. The images were captured under various lighting conditions. The image size is 192 by 168. For computational convenience, the images are resized into 48 by 42. This database can be downloaded from http://vision.ucsd.edu/~leekc/ExtYaleDatabase/ExtYaleB.html (accessed on 18 October 2016).

The AR face database contains 3120 images of 120 subjects, with 26 images per subject. The images were taken with different facial expressions and illuminations, and some images were occluded with black sunglasses or scarves. Here, we use a cropped version of this database where the image size is 50 by 40. This database can be downloaded from http://www2.ece.ohio-state.edu/~aleix/ARdatabase.html (accessed on 18 October 2016).

The Binary Alphadigits database consists of 1404 binary images from 36 classes, with 39 images per class. The images are handwritten digits and letters. Specifically, this database contains digits "0" through "9" and capital letters "A" through "Z". The image size is 20 by 16. This database can be downloaded from http://www.cs.nyu.edu/~roweis/data.html (accessed on 30 September 2018).

The PolyU 3D palmprint database contains 8000 images collected from 400 different palms, with 20 images per palm. Each image contains a 3D region of interest (ROI) and the corresponding 2D ROI. In our experiments, only the 2D ROIs are used. The image size is 128 by 128. For computational convenience, the images are resized into 32 by 32. This database can be downloaded from http://www4.comp.polyu.edu.hk/~biometrics/ (accessed on 9 September 2018).

Table 2 shows the statistics of the four databases. Figure 2 shows some sample images.

Appl. Sci. 2022, 12, 12913 10 of 25

Database	Image Size	No. of Images	No. of Images per Class	No. of Classes
Extended Yale B face	48 × 42	2414	64	38
AR face	50×40	3120	26	120
Binary Alphadigits	20×16	1404	39	36
PolyU 3D palmprint	32×32	8000	20	400

Table 2. The statistics of the four databases used in the experiments.

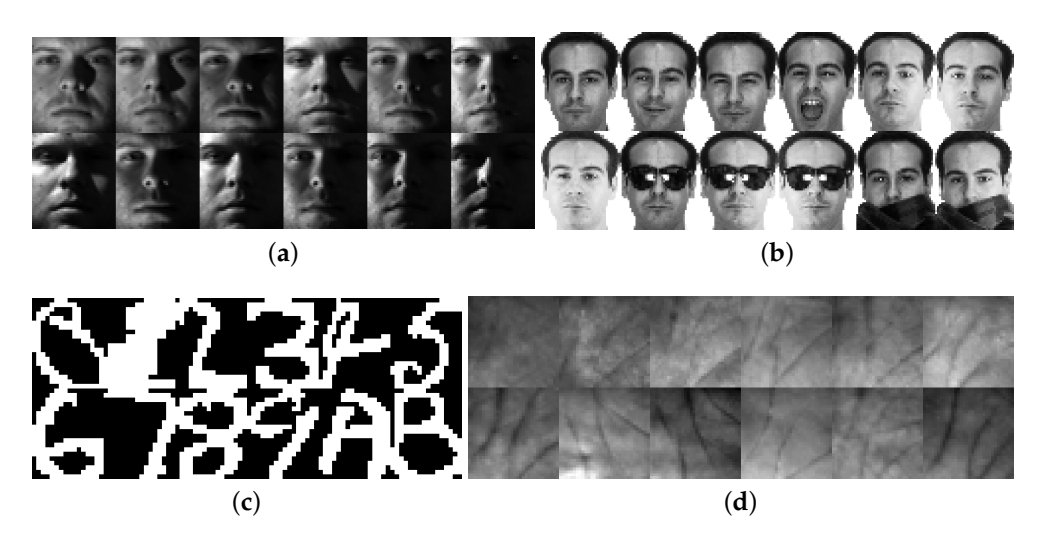


Figure 2. (a) Twelve images of the first subject in the Extended Yale B face database. (b) The first twelve images of the first subject in the AR face database. (c) The first image from twelve different classes in the Binary Alphadigits database. (d) The first image from twelve different classes in the PolyU 3D palmprint database.

4.2. Image Reconstruction

To quantify the comparison of the five algorithms in image reconstruction, we calculate reconstruction errors of these algorithms. Suppose $\mathbf{Z}_i \in \mathbb{R}^{h \times w}$ is the reconstruction image of \mathbf{X}_i by one of the five algorithms, i = 1, 2, ..., n. Then, the average reconstruction error is

$$\frac{1}{n} \sum_{i=1}^{n} \|\mathbf{X}_i - \mathbf{Z}_i\|_F,\tag{19}$$

where $\|\cdot\|_F$ denotes the Frobenius norm. The reconstruction result of PCA is shown in Equation (5). It should be further reshaped into a $h \times w$ matrix in order to obtain the corresponding reconstruction image \mathbf{Z}_i . For the four 2D algorithms, i.e., 2DPCA, A2DPCA, (2D)²PCA and DB2DPCA, their definitions of \mathbf{Z}_i are shown in Equations (9), (13), (15) and (17), respectively. Note that for the two bilateral algorithms, the same number of features are extracted from both laterals.

4.3. Image Recognition

To compare the recognition performance of DB2DPCA with the aforementioned four algorithms, we employ these algorithms to extract features and then apply a specific classifier on the extracted features to perform classification. Since recognition performance is largely determined by the classifier, we try three different classifiers in order to highlight the effects of the feature extraction methods. The classifiers chosen are the Nearest Neighbor (NN) classifier, linear Support Vector Machine (SVM) [62,63] and Collaborative Representation Classifier (CRC) [64,65]. These classifiers are widely employed to evaluate the recognition performance of unsupervised learning algorithms.

Ten-fold cross validation is adopted for performance evaluation—that is, all images are randomly separated into ten folds, wherein nine folds are for training and the remaining

Appl. Sci. 2022, 12, 12913 11 of 25

one fold is for testing. This procedure is repeated ten times and the average classification accuracy is calculated.

For PolyU 3D palmprint database, we perform classification on images from the first 100 subjects to reduce the computational time. For the other three databases, all images are used.

For the two bilateral algorithms, we extract the same number of features from both laterals. To implement linear SVM, we use LibSVM [62,63] with default parameters. As recommended in [62], prior to classification by linear SVM, the training and testing data are linearly scaled. Specifically, each attribute in training data is scaled to [0,1]; then, the same parameters are applied to the testing data. For CRC, the regularization parameter λ is set to be 0.001 * n/700 as in [64], where n is the number of training samples.

4.4. The Effect of Reordering Pixels in Images

All faces, handwritten characters and palmprint images carry semantic information for humans but not for machines. When analyzed by statistical algorithms, an image is essentially a stack of data. Since 2D algorithms treat an image as a whole without transforming it into a long vector, it is natural to ask whether the image structure information affects the classification performances of the above algorithms. To this end, we reorder the pixels in all images of a database by the same rule and then perform classification as described above.

Figure 3 shows sample images from the Extended Yale B face database and six variants generated by reordering the pixels in the original images. For clarity, the original image and its six variants are called variants 0 to 6, respectively. The variants 1 to 4 are generated by rotating the original images by 180 degrees clockwise, flipping the original images upside down, flipping the original images in the left/right direction and exchanging the upper half and lower half of the original images. The remaining two variants are generated by randomly reordering pixels of the original images. These reordering rules are representative. Note that when a reordering rule is chosen, it is applied to the whole database to keep the image structure consistent across all images. Then, we conduct image classification tasks on the reordered databases in order to examine the effect of reordering pixels in images.

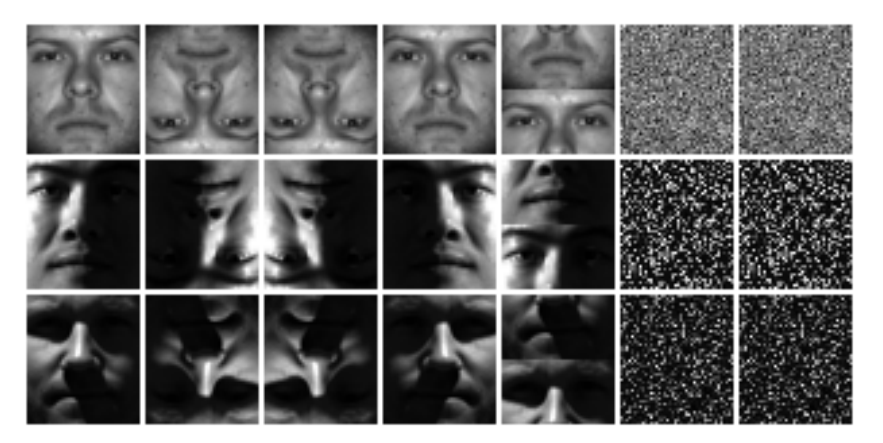


Figure 3. Sample images from the Extended Yale B face database and their variants. The first column shows the sample images and the remaining columns show their variants.

4.5. The Effect of Reshaping Images

As discussed in Section 3.6, DB2DPCA is closely related to other PCA algorithms under some extreme conditions when images are reshaped. Therefore, we proceed to test the effect of reshaping images on classification performances. When an image is reshaped, its structure information is partially lost. In order to preserve the original image structure as much as possible, pixels in the image matrices are stacked column-wise as in Figure 1. By changing the image height p, a series of new databases can be generated. We only

Appl. Sci. 2022, 12, 12913 12 of 25

consider the cases when the image height p satisfies $1 \le p \le \sqrt{d}$ and d is divisible by p. In this way, we can avoid introducing noises in the reshaping procedure.

Since a $p \times q$ image can be reshaped into a $h \times w$ image in many different ways, it is necessary to consider the mixed effects of reordering and reshaping. To this end, we first generate two randomly reordered databases as in Figure 3 and then reshape the reordered databases by stacking pixels column-wise as in Figure 1 to generate two series of new databases. The original database and its reordered and reshaped variants are called variants 0–2 in order. Note that the same reordering and reshaping rule should be applied to all images in the original database in order to keep the image structure consistent. Figure 4 shows the reordered and reshaped images of a sample image from the Extended Yale B face database. The image heights in the eight columns of the figure are 28, 32, 36, 42, 48, 56, 63 and 72 in order.

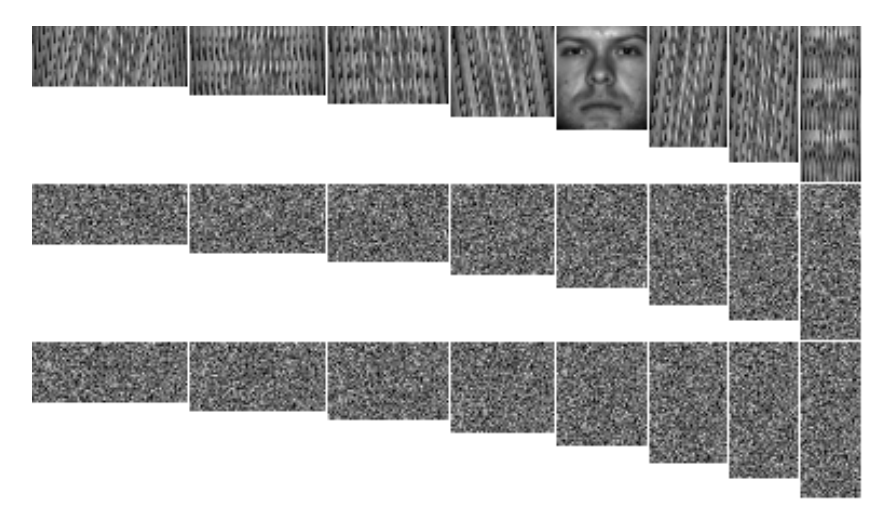


Figure 4. The reordered and reshaped images of a sample image from the Extended Yale B face database. The original image is shown in the fifth column of the first row. The other two images in the fifth column are two randomly reordered variants of this image. In each row, the remaining images are generated by reshaping the fifth image of that row.

For illustration, we focus on the Extended Yale B face database with CRC as the classifier again. Since there are three series of reordered and reshaped databases, we fix the feature number k in the each algorithm as in [21]. Specifically, we choose the smallest k satisfying that the percentage of total variance explained by the first k principal components is larger than a preset threshold θ . The threshold θ is set to 0.5, 0.6, 0.7 and 0.8 in the experiments. For the two bilateral algorithms, i.e., $(2D)^2$ PCA and DB2DPCA, we choose k in the same manner for two laterals separately. Then, we conduct image classification tasks on the reordered and reshaped databases in order to examine the effect of reshaping images.

5. Results

5.1. The Percentage of Total Variance Explained

Before proceeding to the experimental results of image recognition and reconstruction, it is meaningful to examine the percentages of total variance explained by features of different algorithms. This can provides valuable insights on the differences between the three basic types of PCA transformations, i.e., PCA, 2DPCA and A2DPCA. The principal components of two bilateral 2D algorithms, i.e., $(2D)^2$ PCA and DB2DPCA, are directly inherited from the two unilateral 2D algorithms. Thus, it is not necessary to analyze them separately.

Table 3 shows the maximal number of principal components that can be extracted by different algorithms. Since there are plenty of samples in the four databases, as shown

in Table 2, the maximal number of principal components that can be extracted by PCA, 2DPCA and A2DPCA equals the image size, image width and image height, respectively.

Table 3. The maxima	l number of princ	cipal components	extracted by	different algorithms.

Database	PCA	2DPCA	A2DPCA
Extended Yale B face	2016	42	48
AR face	2000	40	50
Binary Alphadigits	320	16	20
PolyU 3D palmprint	1024	32	32

Figure 5 shows the percentages of total variance explained by the first thirty principal components of the three algorithms. For the Binary Alphadigits database, the results corresponding to the maximal number of principal components are calculated. Detailed results when the number of principal components is smaller than seven are listed in Table 4. The results of the two unilateral 2D algorithms are exactly the same, and both are much larger than the corresponding results of PCA. For the two unilateral 2D algorithms, the first thirty principal components can explain most of the total variance. For PCA, the first thirty principal components can explain 70% to 97% of the total variance, depending on the database. The percentages of total variance explained indicate how much information is extracted from a specific database, thus greatly affecting the performances of the feature extraction algorithms in image reconstruction and recognition.

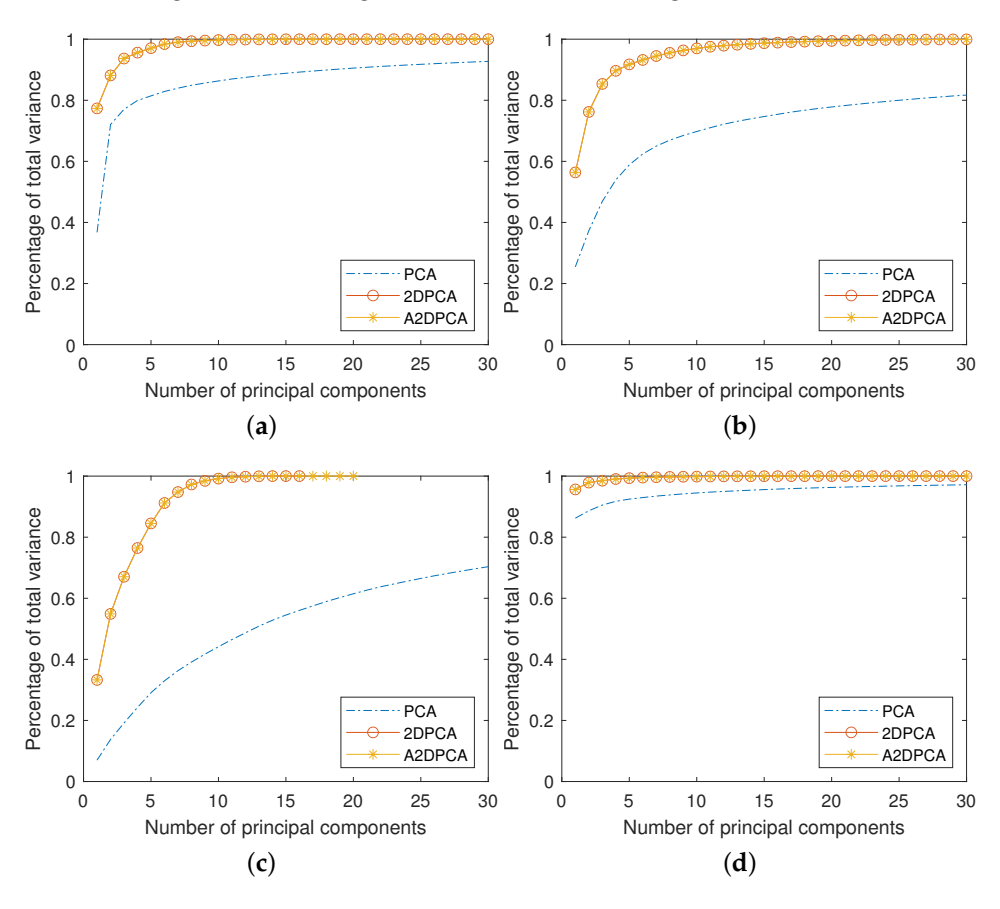


Figure 5. The percentages of total variance explained by the first thirty principal components. (a) Extended Yale B face database. (b) AR face database. (c) Binary Alphadigits database. (d) PolyU 3D palmprint database.

Database	Algorithm		Numl	er of Princ	ipal Compo	onents	
Database	Algorithm	1	2	3	4	5	6
	PCA	0.3674	0.7206	0.7705	0.7993	0.8144	0.8288
Extended Yale B face	2DPCA	0.7734	0.8813	0.9367	0.9560	0.9708	0.9840
	A2DPCA	0.7734	0.8813	0.9367	0.9560	0.9708	0.9840
	PCA	0.2545	0.3727	0.4688	0.5393	0.5885	0.6242
AR face	2DPCA	0.5638	0.7618	0.8535	0.8964	0.9175	0.9320
	A2DPCA	0.5638	0.7618	0.8535	0.8964	0.9175	0.9320
	PCA	0.0699	0.1378	0.1917	0.2426	0.2909	0.3298
Binary Alphadigits	2DPCA	0.3327	0.5488	0.6705	0.7645	0.8451	0.9119
, 1	A2DPCA	0.3327	0.5488	0.6705	0.7645	0.8451	0.9119
	PCA	0.8622	0.8864	0.9052	0.9175	0.9247	0.9298
PolyU 3D palmprint	2DPCA	0.9563	0.9788	0.9849	0.9905	0.9932	0.9950
roly c ob pulliprint	A2DPCA	0.9563	0.9788	0.9849	0.9905	0.9932	0.9950

Table 4. The percentages of total variance explained by the first six principal components.

5.2. Image Reconstruction

Figure 6 shows the reconstructed images of the five algorithms, wherein the first ten feature vectors are used for image reconstruction. Note that for the two bilateral algorithms, the first ten projection vectors from both laterals are used. The reconstructed images of PCA and (2D)²PCA are very obscure. The reconstructed images of 2DPCA and A2DPCA have vertical stripes and horizontal stripes, respectively. The reconstructed images of DB2DPCA highly approximate the original images. Obviously, the proposed algorithm outperforms the other four algorithms in image reconstruction.

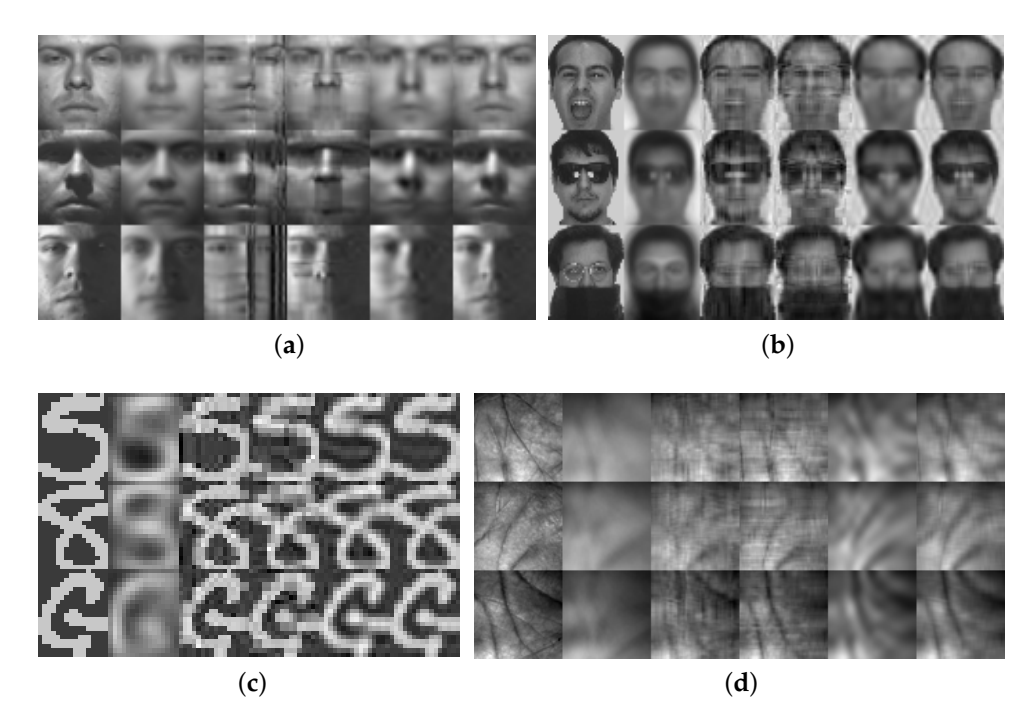


Figure 6. The reconstructed images of the five algorithms. In each subfigure, the first column shows the original images while the remaining columns show the reconstructed images of PCA, 2DPCA, A2DPCA, (2D)²PCA and DB2DPCA, respectively. (a) Extended Yale B face database. (b) AR face database. (c) Binary Alphadigits database. (d) PolyU 3D palmprint databse.

Figure 7 shows the average reconstruction errors of the five algorithms with different numbers of extracted features. For the two bilateral algorithms, we select the same number of features for both laterals. By averaging the results in Figure 7 across different feature numbers, we obtain Table 5. With the exception of Figure 7a, the average reconstruction errors of PCA are the largest among the five algorithms, the average reconstruction errors of DB2DPCA are the smallest and the results of the other three algorithms lie between those

Appl. Sci. 2022, 12, 12913 15 of 25

of PCA and DB2DPCA. These results again demonstrate that DB2DPCA outperforms the other four algorithms in image reconstruction.

It is not surprising that the reconstructed images of PCA are very obscure and the average reconstruction errors of PCA are large. The maximal number of principal components that can be extracted by PCA is much larger than those of the two unilateral algorithms, as shown in Table 3, but only the first few feature vectors are used to generate the reconstructed image or calculate the reconstruction errors. The percentages of total variance explained by these feature vectors are relatively small, as shown in Figure 5 and Table 4, and cannot be guaranteed to reconstruct the original image accurately. By comparison, the total number of features that can be extracted by 2DPCA-based algorithms is small and the percentage of total variance explained by the same number of feature vectors of these algorithms is large. Therefore, 2DPCA-based algorithms perform much better than PCA with the same number of feature vectors in image reconstruction.

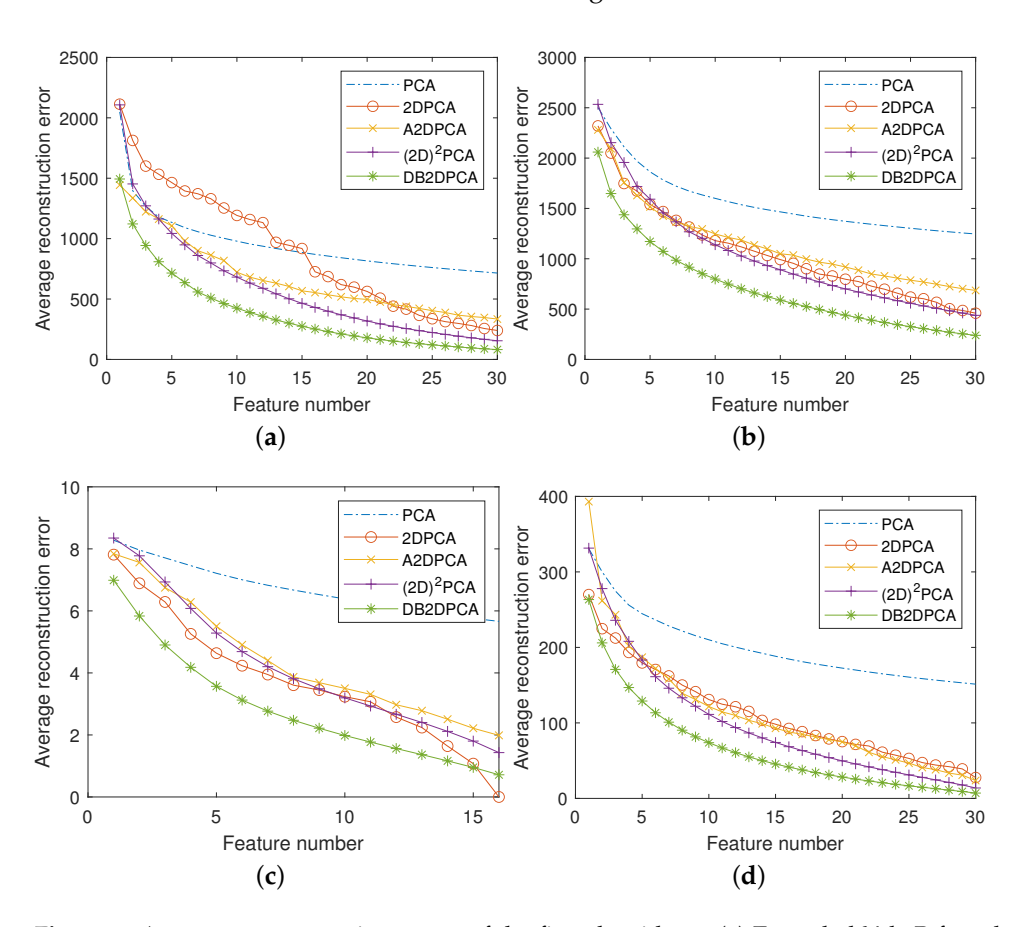


Figure 7. Average reconstruction errors of the five algorithms. (a) Extended Yale B face database. (b) AR face database. (c) Binary Alphadigits database. (d) PolyU 3D palmprint databse.

Table 5. Average reconstruction errors of the five algorithms on four databases.

Database	PCA	2DPCA	A2DPCA	$(2D)^2$ PCA	BD2DPCA
Extended Yale B face	952.2	894.4	676.2	594.5	385.8
AR face	1557.9	1056.9	1142.0	1021.2	708.1
Binary Alphadigits	6.9	4.2	4.7	4.6	3.1
PolyU 3D palmprint	199.7	111.0	112.9	97.9	66.2

The reconstructed images of 2DPCA and A2DPCA have vertical stripes and horizontal stripes, respectively. The average reconstruction errors of the two unilateral algorithms are much larger than those of DB2DPCA; this is because 2DPCA only projects the rows of images onto its projection matrix and A2DPCA only projects the columns of images onto

Appl. Sci. 2022, 12, 12913 16 of 25

its projection matrix. Since the noises in the reconstructed images of 2DPCA and A2DPCA exist in different directions, these noises counteract with each other when they are averaged by DB2DPCA. Therefore, DB2DPCA has better reconstruction performance than the two unilateral 2D algorithms.

The reconstructed images of $(2D)^2PCA$ are also obscure. The average reconstruction errors of $(2D)^2PCA$ are much larger than those of DB2DPCA; this is because $(2D)^2PCA$ projects the rows and columns of images onto the corresponding projection matrices simultaneously, thus mixing bilateral information together and leading to information loss. DB2DPCA avoids this problem by averaging between the reconstruction results of the two unilateral algorithms, thus strengthening their similarities and weakening their differences. Therefore, DB2DPCA achieves better image reconstruction performance than $(2D)^2PCA$.

The reconstructed images of DB2DPCA highly approximate the original images, and the average reconstruction errors of DB2DPCA are the smallest among the five algorithms. Therefore, we conclude that DB2DPCA outperforms the other four algorithms in image reconstruction.

In recent years, ℓ_1 -norm and ℓ_p -norm were introduced to improve 2DPCA algorithms, proposing new algorithms such as 2DPCA-L1 [27], 2DPCAL1-S [30] and G2DPCA [31]. These algorithms are expected to be more robust to noise and obtain sparse results. However, they only slightly outperform 2DPCA in image reconstruction even with optimal tuning parameters, especially when the feature number is small. Compared with these algorithms, DB2DPCA is rather efficacious in image reconstruction.

5.3. Image Recognition

Figure 8 shows the average classification accuracies of the five algorithms followed by three different classifiers on four databases. By averaging the results in Figure 8 across different feature numbers, we obtain Table 6. PCA underperforms compared with 2DPCA-based algorithms in most cases. The reason is similar to that discussed in Section 5.2. With the exceptions of Figure 8a,d,i, DB2DPCA obtains the highest classification accuracies among the five algorithms.

Two exceptions where 2DPCA outperforms DB2DPCA exist in Figure 8a,d, in which cases the classifier is chosen to be NN. The accuracies of NN in both cases are much lower than corresponding results of SVM and CRC in Figure 8b,c,e,f where DB2DPCA outperforms 2DPCA. Therefore, we conclude that NN cannot make the most of the information extracted by DB2DPCA in the two cases.

Comparing between the two bilateral 2D algorithms, DB2DPCA outperforms $(2D)^2$ PCA in most cases. The only exception occurs on the Binary Alphadigits database in Figure 8i, when CRC is applied as the classifier and the feature number is larger than four. The reason might be that the image size of the Binary Alphadigits database is much smaller than the other three databases. With the exception of Figure 8i, DB2DPCA greatly outperforms $(2D)^2$ PCA in image recognition. It is also due to the fact that $(2D)^2$ PCA projects the rows and columns of images onto the corresponding projection matrices simultaneously, thus mixing bilateral information together and leading to information loss. On the other side, DB2DPCA concatenates bilateral information directly and extracts more features that can improve the image recognition performance.

The curves of the four 2D algorithms on the Binary Alphadigits database in Figure 8g–i are different from the corresponding curves in other figures in that they do not monotonically increase with feature number; this is because the image size of the Binary Alphadigits database (20×16) is much smaller than those of the other three databases. Since we extract at most 16 features for this database, there exist redundant features when the feature number is large. The redundant features deteriorate the classification performances. For the other three databases, the maximal feature number is much smaller than the image size of the databases; so, their classification accuracies tend to increase with feature number. If we focus on the results when the feature number is small and no redundant features are extracted, DB2DPCA has obvious advantages over competing algorithms.

Appl. Sci. 2022, 12, 12913 17 of 25

Since DB2DPCA can make the most of bilateral information from images, it is natural that DB2DPCA generally outperforms the other four algorithms in image classification.

Based on the results in Table 6, it is straightforward to compare classification performances among the three classifiers. CRC greatly outperforms the other two classifiers on the Extended Yale B face database; SVM greatly outperforms the other two classifiers on the AR face database; SVM slightly outperforms NN on the Binary Alphadigits database; NN greatly outperforms the other two classifiers on the PolyU 3D palmprint database. Therefore, no classifier has an absolute advantage over the others.

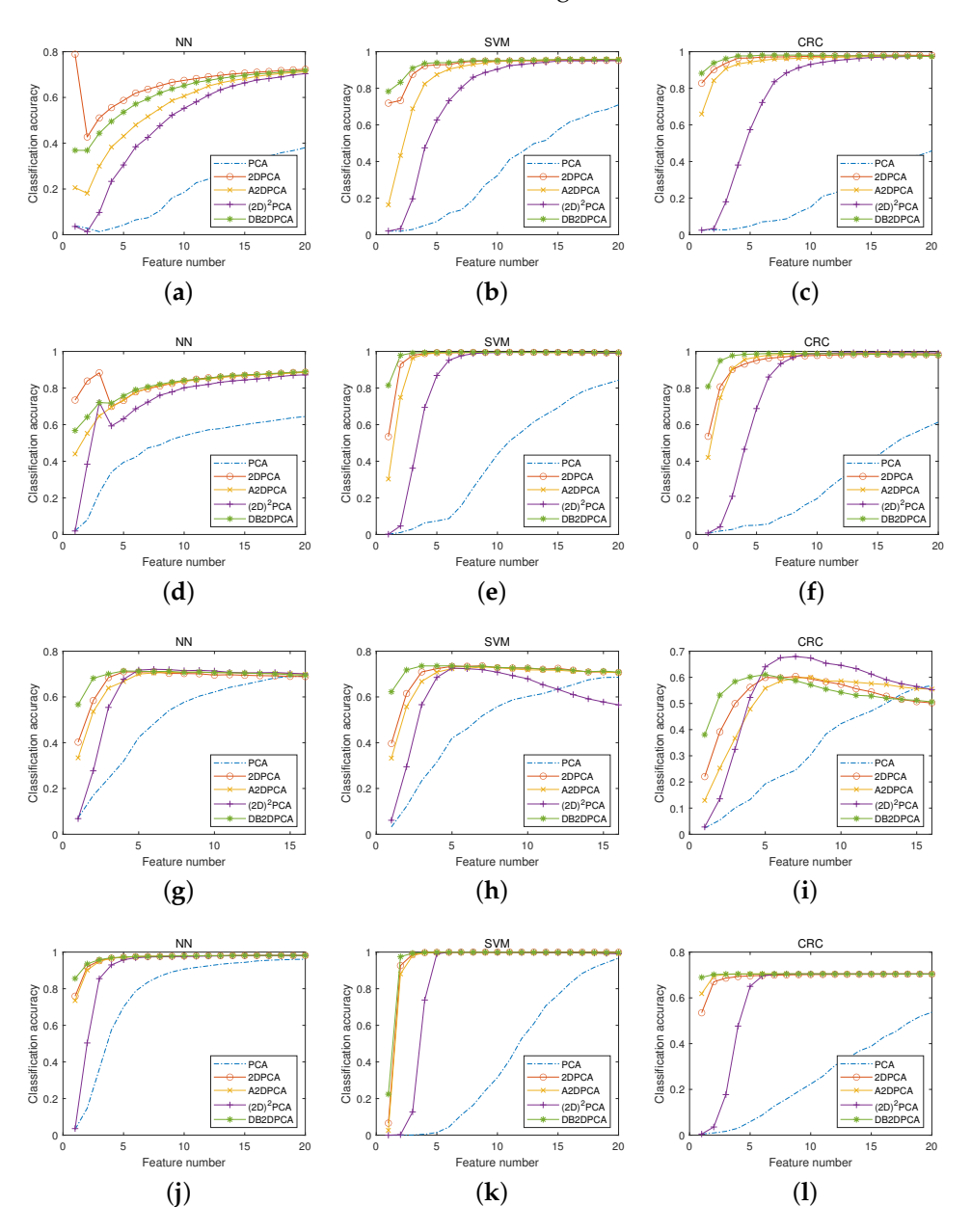


Figure 8. The average classification accuracies on four databases by three different classifiers. The subfigures in the four rows are results of the Extended Yale B face database, AR face database, Binary Alphadigits database and PolyU 3D palmprint database, respectively. The subfigures (**a–l**) in three columns are results of NN, linear SVM and CRC, respectively. In each subfigure, there are five accuracy curves corresponding to the five feature extraction algorithms, i.e., PCA, 2DPCA, A2DPCA, $(2D)^2$ PCA and DB2DPCA.

Database	Classifier	PCA	2DPCA	A2DPCA	(2D) ² PCA	DB2DPCA
	NN	0.2716	0.6835	0.6111	0.5621	0.6515
Extended Yale B face	SVM	0.4922	0.9306	0.8930	0.8171	0.9426
	CRC	0.3316	0.9669	0.9524	0.8302	0.9669
	NN	0.5459	0.8517	0.8236	0.7806	0.8378
AR face	SVM	0.5892	0.9745	0.9588	0.8877	0.9870
	CRC	0.4196	0.9531	0.9555	0.8655	0.9738
	NN	0.5050	0.6724	0.6643	0.6318	0.6954
Binary Alphadigits	SVM	0.4873	0.6947	0.6805	0.5931	0.7179
, ,	CRC	0.3226	0.5235	0.5089	0.5317	0.5422
	NN	0.8411	0.9693	0.9677	0.9256	0.9739
PolyU 3D palmprint	SVM	0.6123	0.9650	0.9567	0.8888	0.9707
, , ,	CRC	0.3723	0.6949	0.7014	0.6316	0.7034

Table 6. The average classification accuracies on four databases by three different classifiers.

5.4. The Effect of Reordering Pixels in Images

For illustration of the effect of reordering pixels in images, we focus on the Extended Yale B face database with CRC as the classifier. Similar experiments have been conducted on the original database and the results are shown in Figure 8c. Therefore, in the current experiment, we emphasize the effect of reordering pixels in images rather than the comparison between different feature extraction algorithms.

Figure 9 shows the average classification accuracies on the Extended Yale B face database and its six reordered variants. For illustration, only the results when the feature number is smaller than 11 are displayed. As an example of the detailed results, Table 7 shows the accuracies when only the first two features are used to perform classification.

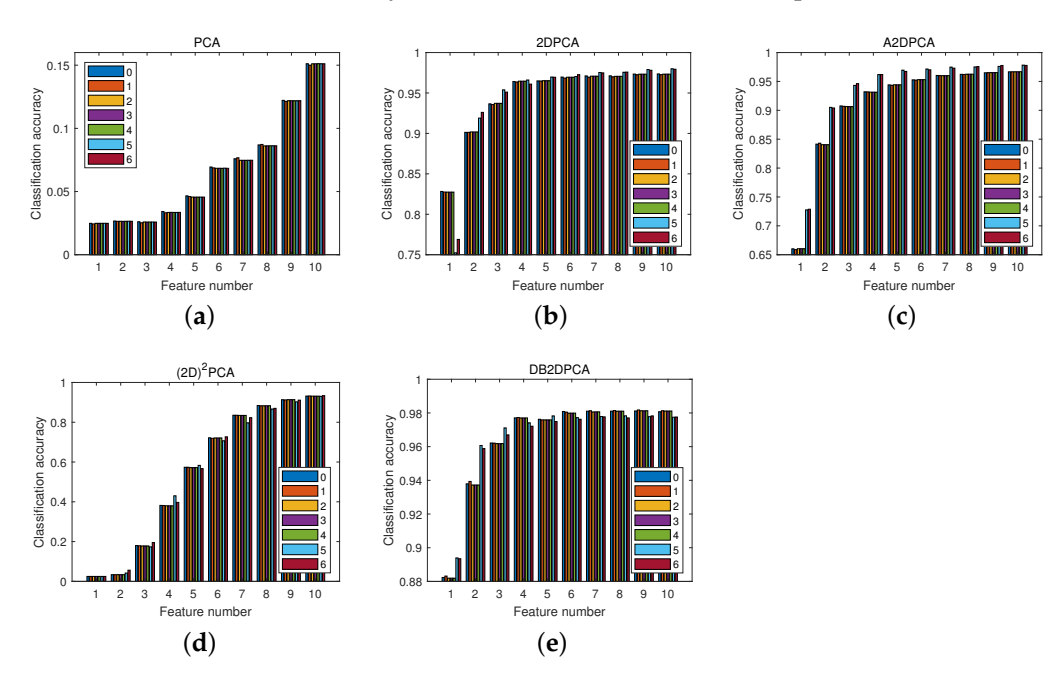


Figure 9. The average classification accuracies on Extended Yale B face database and its six reordered databases with CRC as the classifier. (a) PCA. (b) 2DPCA. (c) A2DPCA. (d) (2D)²PCA. (e) DB2DPCA.

The accuracies of PCA are very close among the variants; this is due to the fact that PCA does not incorporate 2D image structure during the feature extraction procedure. For the other four algorithms, the results on variants 0–4 are very close to each other while the results on variants 5–6 tend to be quite different; this is because variants 0–4 preserve the original image structure but variants 5–6 only have random image structures. Therefore, reordering pixels in images can affect the classification performances of the 2D algorithms. In other words, the image structure information is incorporated in the feature extraction procedure of the 2D algorithms.

Appl. Sci. 2022, 12, 12913 19 of 25

Table 7. The average classification accuracies on the Extended Yale B face database and its six reordered databases with CRC as the classifier when only the first two features are used to perform classification.

Variant	PCA	2DPCA	A2DPCA	(2D) ² PCA	DB2DPCA
0	0.0267	0.9013	0.8415	0.0336	0.9379
1	0.0264	0.9013	0.8431	0.0335	0.9394
2	0.0265	0.9018	0.8405	0.0338	0.9372
3	0.0264	0.9018	0.8405	0.0338	0.9372
4	0.0265	0.9018	0.8405	0.0338	0.9372
5	0.0265	0.9189	0.9051	0.0419	0.9607
6	0.0265	0.9260	0.9040	0.0562	0.9588

5.5. The Effect of Reshaping Images

Figure 10 shows the average classification accuracies with different image heights and different thresholds θ on the Extended Yale B face database and its reordered and reshaped variants. Specifically, the three columns show the results corresponding to the three series of modified databases, i.e., variants 0–2 in order, and the four rows show the results corresponding to the four thresholds in order. The classifier is chosen to be CRC for illustration. By averaging the results in Figure 10 across different image heights, we obtain Table 8.

The experiments corresponding to the three columns in Figure 10 differ in the way of reordering pixels in images. It again demonstrates that reordering pixels in images will affect the classification performances of the four 2D algorithms. The results on variants 1–2 (column 2–3) are much better than the results on variant 0 (column 1). The reason might be that the features extracted from the original images contain more redundant information than the features extracted from the randomly reordered and reshaped images. In other words, by randomly reordering the pixels in images and reshaping the image size, we can extract more valuable information that can improve the classification performance.

In the first column of Figure 10, the accuracy of 2DPCA generally increases with image height and the accuracy of A2DPCA generally decreases with image height. The reason is that 2DPCA projects the rows of images onto its projection matrix while A2DPCA projects the columns of images onto its projection matrix. As a result, the number of features extracted by 2DPCA increases with image height and the number of features extracted by A2DPCA decreases with image height. More features generally indicate higher classification accuracies, especially when the percentage of total variance explained by these features is small. Therefore, the accuracy of 2DPCA generally increases with image height and the accuracy of A2DPCA generally decreases with image height in the first column of Figure 10. This is not the case in the last two columns since the reordering and reshaping effect dominates these results.

The accuracies of DB2DPCA are rather stable with different image heights in all cases in Figure 10; this is because that DB2DPCA can extract features from both laterals of images. In this way, it inherits the advantages of 2DPCA and A2DPCA, and can achieve high classification accuracies with different image heights. From Table 8, DB2DPCA greatly outperforms competing algorithms except A2DPCA on all of the three variants. To be specific, DB2DPCA is significantly better than A2DPCA on variant 0 and slightly worse than A2DPCA on variants 1–2. The reason why DB2DPCA is slightly worse than A2DPCA on variants 1–2 might be that the features extracted from the randomly reordered and reshaped images by A2DPCA are sufficient for image classification, and extracting more features by DB2DPCA introduces redundant information that deteriorates the classification performances. Generally speaking, DB2DPCA achieves the best classification performances among the five competing algorithms on the reordered and reshaped images.

Appl. Sci. 2022, 12, 12913 20 of 25

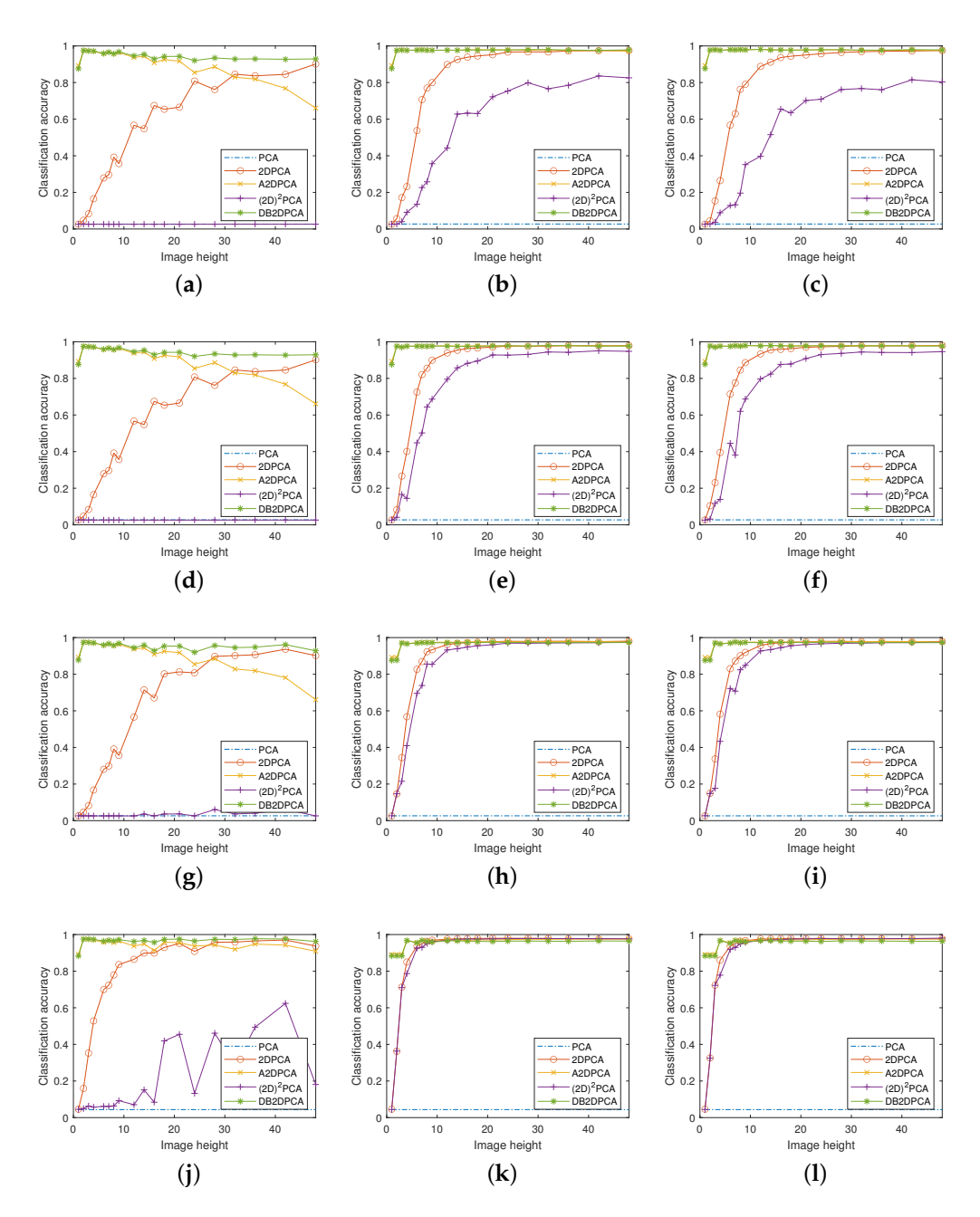


Figure 10. The average classification accuracies corresponding to four thresholds on the Extended Yale B face database and its reordered and reshaped variants with CRC as the classifier. Four rows correspond to results when the threshold θ equals 0.5, 0.6, 0.7 and 0.8 in order. Three columns correspond to results of variants 0–2 in order. In each subfigure (**a–1**), the five accuracy curves correspond to the five feature extraction algorithms, i.e., PCA, 2DPCA, A2DPCA, (2D)²PCA and DB2DPCA.

The experiments corresponding to the four rows in Figure 10 differ in the preset θ value. Generally speaking, the classification accuracies increase with increasing θ value; this is due to the fact that the number of extracted features increases when the percentage of total variance explained by these features—i.e., the θ value—increases. Having more features leads to better classification performance, especially when the percentage of total variance explained by these features is not large enough, e.g., smaller than 0.95. Therefore, the classification accuracies increase with increasing θ value.

Table 8. The average classification accuracies corresponding to four thresholds on the Extended Yale
B face database and its reordered and reshaped variants with CRC as the classifier.

θ	Variant	PCA	2DPCA	A2DPCA	$(2D)^2$ PCA	DB2DPCA
	0	0.0268	0.5134	0.9003	0.0261	0.9436
0.5	1	0.0272	0.7254	0.9726	0.4727	0.9722
	2	0.0272	0.7199	0.9736	0.4478	0.9732
	0	0.0272	0.5133	0.9003	0.0260	0.9434
0.6	1	0.0272	0.7755	0.9724	0.6662	0.9709
	2	0.0272	0.7694	0.9737	0.6510	0.9717
	0	0.0266	0.5562	0.9008	0.0328	0.9498
0.7	1	0.0265	0.8090	0.9668	0.7635	0.9620
	2	0.0263	0.8071	0.9666	0.7598	0.9625
	0	0.0438	0.7561	0.9456	0.2027	0.9654
0.8	1	0.0438	0.8708	0.9576	0.8637	0.9510
	2	0.0438	0.8698	0.9579	0.8608	0.9509

Figure 10 exhibits the classification performances of the four 2D algorithms only when $p < \sqrt{d}$. Based on symmetries of these algorithms, their classification performances when $p > \sqrt{d}$ can be directly inferred. Let c be an arbitrary divisor of d; then, 2DPCA with p = c approximates to A2DPCA with p = d/c, $(2D)^2$ PCA with p = c approximates to $(2D)^2$ PCA with p = d/c, and DB2DPCA with p = d/c. Consequently, we can further conclude that DB2PCA can achieve the best classification performances among the five competing algorithms when the image height p is in the full range of [1,d].

6. Discussion

6.1. Other Comparisons

Five algorithms, as listed in Table 9, are fully compared in the experiments. Considering that the mechanisms of PCA- and 2DPCA-based algorithms are quite different, as discussed in Section 5.1, and that the unilateral algorithms only extract features from a single lateral of images while the bilateral algorithms extract features from both laterals of images, it is not very fair to compare the five feature extraction algorithms directly using the same number of feature vectors. Strictly speaking, fair comparisons can be made only between the two unilateral algorithms, or between the two bilateral algorithms.

Table 9. Five algorithms compared in the experiments.

Category	Bibliography	Algorithm
1D	Turk and Pentland [11]	PCA
Unilateral 2D	Yang et al. [13]	2DPCA
Unilateral 2D	Zhang and Zhou [21]	A2DPCA
Bilateral 2D	Zhang and Zhou [21]	$(2D)^2$ PCA
Bilateral 2D	Proposed	DB2DPCA

By comparing between the two unilateral algorithms, 2DPCA generally outperforms A2DPCA both in image reconstruction and recognition, as shown in Figures 7–9 and Tables 5–7. However, A2DPCA greatly outperforms 2DPCA on the reshaped databases, as shown in Figure 10 and Table 8. As we know, 2DPCA with p=c approximates to A2DPCA with p=d/c. The comparison of 2DPCA and A2DPCA is directly influenced by the ratio of image height to image width. Since the image height is commonly larger than the image width on the four databases, 2DPCA can extract more information than A2DPCA with the same feature number. Therefore, 2DPCA generally performs better than A2DPCA. However, in the reshaped databases, the image height might be much smaller than the image width. In these cases, A2DPCA generally performs better than 2DPCA.

When the image height equals the image width, the performances of 2DPCA and A2DPCA are very close.

By comparing between the two bilateral algorithms, DB2DPCA significantly outperforms $(2D)^2$ PCA in all experiments. The main reason is that $(2D)^2$ PCA projects the rows and columns of images onto two lateral eigenvectors simultaneously, thus mixing bilateral information together and leading to information loss. In contrast, DB2DPCA projects the rows and columns of images onto two lateral eigenvectors separately, thus extracting more features from images and obtaining a more interpretable reconstruction model. Therefore, DB2DPCA performs better than $(2D)^2$ PCA both in image reconstruction and recognition.

6.2. Limitations of DB2DPCA

Despite the above advantages, DB2DPCA has some limitations. First, since DB2DPCA is rooted in 2DPCA and A2DPCA, to calculate the feature matrices or the reconstruction images for DB2DPCA, we need to calculate the corresponding results for 2DPCA and A2DPCA first, which is time consuming. However, other bilateral algorithms such as $(2D)^2$ PCA also suffer from a similar problem. Second, since the original image height h and image width w are usually much larger than the feature numbers k and l, the sizes of the feature matrices of DB2DPCA tend to be much larger than those of the other three 2D algorithms. This is a major disadvantage of DB2DPCA. There are three folds of meanings to this disadvantage: (1) DB2DPCA needs a larger coefficient set for image representation than other 2D algorithms. (2) It will take longer to perform image classification by DB2DPCA than by the other three 2D algorithms; therefore, the good classification performances of DB2DPCA are obtained at the sacrifice of computational efforts. (3) There exist redundancies by pooling bilateral information together. This may explain why DB2DPCA underperforms compared with 2DPCA in face recognition in Figure 8a,d.

6.3. Future Directions

From a certain perspective, 2DPCA-based algorithms outperform PCA because they preserve the image spatial structure by treating the images as 2D matrices rather than reshaping them into 1D vectors. To further exploit the image spatial structure, we can introduce a spatial structure regularization [66] into the 2DPCA-based algorithms. This is expected to improve their performances in image analysis.

Most of the algorithms in Table 1 are built on traditional unilateral 2DPCA, and can be improved by implementing the direct bilateral idea. Intuitively, this idea can make full use of bilateral information of images for unilateral 2D feature extraction methods, unilateral 2D manifold learning methods and their variants [67,68], thus improving their performances.

7. Conclusions

This paper proposes a novel bilateral 2DPCA algorithm named DB2DPCA for image reconstruction and recognition, which fuses bilateral information of images in a direct manner. For image recognition, the projection result of DB2DPCA is calculated by concatenating the projection results of two unilateral 2D algorithms, i.e., 2DPCA and A2DPCA. Therefore, it can extract more features, which are useful for image recognition. For image reconstruction, the reconstruction result of DB2DPCA is calculated by averaging the reconstruction results of the two unilateral algorithms. In this way, it strengthens their common parts and weakens their differences, thus reconstructing the original image accurately. To evaluate the proposed algorithm, we compare it with four related feature extraction algorithms in the tasks of image reconstruction and recognition. Four benchmark databases are used and three different classifiers are tested in the experiments. As a result, DB2DPCA generally outperforms competing algorithms both in image reconstruction and recognition. Additional experiments on reordered and reshaped databases further demonstrate the superiority of the proposed algorithm. In conclusion, DB2DPCA is an effective algorithm for image reconstruction and recognition. The direct bilateral idea can be applied to other unilateral 2D algorithms to improve their performances in image analysis.

Appl. Sci. 2022, 12, 12913 23 of 25

Author Contributions: Conceptualization, J.W.; methodology, J.W.; validation, M.Z., X.X. and L.Z.; writing—original draft preparation, J.W., L.Z. and W.Z.; writing—review and editing, L.Z. and W.Z.; funding acquisition, J.W., L.Z. and W.Z. All authors have read and agreed to the published version of the manuscript.

Funding: This research was funded in part by the National Natural Science Foundation of China under Grant 31900710; in part by the Key Scientific Research Projects of Henan Province under Grant 22A520008 and Grant 22A520007; in part by the Natural Science Foundation of Henan Province under Grant 222300420275 and Grant 222300420274; in part by the Youth Scientific Research Fund Project of Xinyang Normal University under Grant 2021-QN-036; and in part by the Nanhu Scholars Program for Young Scholars of Xinyang Normal University.

Institutional Review Board Statement: Not applicable.

Informed Consent Statement: Not applicable.

Data Availability Statement: Not applicable.

Conflicts of Interest: The authors declare no conflict of interest.

References

1. Khalid, S.; Khalil, T.; Nasreen, S. A survey of feature selection and feature extraction techniques in machine learning. In Proceedings of the 2014 Science and Information Conference, London, UK, 27–29 August 2014; pp. 372–378.

- 2. Saini, S.; Malhotra, P. A Comprehensive Survey of Feature Extraction and Feature Selection Techniques of Face Recognition System. In Proceedings of the Fist International Conference on Advanced Scientific Innovation in Science, Engineering and Technology, ICASISET 2020, Chennai, India, 16–17 May 2020; EAI: Gent, Belgium, 2021.
- 3. Gill, R.; Singh, J. A Review of Feature Extraction Techniques for EEG-Based Emotion Recognition System. In *Soft Computing: Theories and Applications*; Advances in Intelligent Systems and Computing; Springer: Singapore, 2021.
- 4. Li, H. Research Review of Feature Extraction and Classification Recognition of Rice Disease Images based on Computer Vision Technology. *J. Phys. Conf. Ser.* **2020**, *1544*, 012116. [CrossRef]
- 5. Kumari, N.; Bhatia, R. Systematic review of various feature extraction techniques for facial emotion recognition system. *Int. J. Intell. Eng. Inform.* **2021**, *9*, 59–87. [CrossRef]
- 6. Bouziane, A.; Kharroubi, J.; Zarghili, A. Towards an objective comparison of feature extraction techniques for automatic speaker recognition systems. *Bull. Electr. Eng. Inform.* **2021**, *10*, 374–382. [CrossRef]
- 7. Mohammed, M.A.; Abdulkareem, K.H.; Garcia-Zapirain, B.; Mostafa, S.A.; Maashi, M.S.; Al-Waisy, A.S.; Subhi, M.A.; Mutlag, A.A.; Le, D.N. A Comprehensive Investigation of Machine Learning Feature Extraction and Classification Methods for Automated Diagnosis of COVID-19 Based on X-Ray Images. *Comput. Mater. Contin.* **2021**, *66*, 3289–3310. [CrossRef]
- 8. Subramani, P.; Srinivas, K.; Kavitha Rani, B.; Sujatha, R.; Parameshachari, B.D. Prediction of muscular paralysis disease based on hybrid feature extraction with machine learning technique for COVID-19 and post-COVID-19 patients. *Pers. Ubiquitous Comput.* **2021**, 1–14. [CrossRef]
- 9. Shlens, J. A Tutorial on Principal Component Analysis. *arXiv* **2014**, arXiv:1404.1100.
- 10. Jolliffe, I.T.; Cadima, J. Principal component analysis: A review and recent developments. *Philos. Trans. R. Soc. A Math. Phys. Eng. Sci.* **2016**, 374, 20150202. [CrossRef]
- 11. Turk, M.A.; Pentland, A.P. Face recognition using eigenfaces. In Proceedings of the IEEE Conference on Computer Vision and Pattern Recognition, Shanghai, China, 11–13 March 1991; pp. 586–591.
- 12. Mitchell-Heggs, R.; Prado, S.; Gava, G.P.; Go, M.A.; Schultz, S.R. Neural manifold analysis of brain circuit dynamics in health and disease. *arXiv* 2022, arXiv:2203.11874.
- 13. Yang, J.; Zhang, D.; Frangi, A.F.; Yang, J.Y. Two-dimensional PCA: A new approach to appearance-based face representation and recognition. *IEEE Trans. Pattern Anal. Mach. Intell.* **2004**, *26*, 131–137. [CrossRef]
- 14. Khan, A.; Jalal, A.S. A Visual Saliency-Based Approach for Content-Based Image Retrieval. *Int. J. Cogn. Inform. Nat. Intell.* **2021**, 15, 1–15. [CrossRef]
- 15. Yin, X.; Chen, L. A Cross-Modal Image and Text Retrieval Method Based on Efficient Feature Extraction and Interactive Learning CAE. Sci. Program. 2022, 2022, 7314599. [CrossRef]
- 16. Ma, X.; Luo, Y.; Shi, J.; Xiong, H. Acoustic Emission Based Fault Detection of Substation Power Transformer. *Appl. Sci.* **2022**, 12, 2759. [CrossRef]
- 17. Garg, M.; Arora, A.S.; Gupta, S. An Efficient Human Identification Through Iris Recognition System. *J. Signal Process. Syst.* **2021**, 93, 701–708. [CrossRef]
- 18. Xu, R.; Li, D. Automatic Target Recognition Technology of SAR Images Based on 2DPCA+PNN. *J. Phys. Conf. Ser.* **2020**, 1626, 012108. [CrossRef]
- 19. Qiu, M.; Zhao, Z. Bearing fault diagnosis using a novel coding-statistic feature combined with NNC. *J. Vibroengineering* **2022**, 24, 848–861. [CrossRef]

20. Warsun, A.; Putra, A.T. Diagnosis Using Brain Tumors Two-Dimensional Principal Component Analysis (2D-PCA) with K-nearest Neighbor (KNN) Classification Algorithm. *J. Adv. Inf. Syst. Technol.* **2021**, *3*, 17–24. [CrossRef]

- 21. Zhang, D.; Zhou, Z.H. (2D)²PCA: Two-directional two-dimensional PCA for efficient face representation and recognition. *Neurocomputing* **2005**, *69*, 224–231. [CrossRef]
- 22. Kong, H.; Wang, L.; Teoh, E.K.; Li, X.; Wang, J.G.; Venkateswarlu, R. Generalized 2D principal component analysis for face image representation and recognition. *Neural Netw.* **2005**, *18*, 585–594. [CrossRef]
- Yang, W.; Sun, C.; Ricanek, K. Sequential Row-Column 2DPCA for face recognition. Neural Comput. Appl. 2012, 21, 1729–1735.
- 24. Titijaroonroj, T.; Hancherngchai, K.; Rungrattanaubol, J. Regional Covariance Matrix-Based Two-Dimensional PCA for Face Recognition. In Proceedings of the 2020 12th International Conference on Knowledge and Smart Technology (KST), Pattaya, Thailand, 29 January–1 February 2020; pp. 6–11.
- 25. Sahoo, T.K.; Banka, H.; Negi, A. Novel approaches to one-directional two-dimensional principal component analysis in hybrid pattern framework. *Neural Comput. Appl.* **2020**, *32*, 4897–4918. [CrossRef]
- 26. Sahoo, T.K.; Banka, H.; Negi, A. Design and analysis of various bidirectional 2DPCAs in feature partitioning framework. *Multimed. Tools Appl.* **2021**, *80*, 24491–24531. [CrossRef]
- 27. Li, X.; Pang, Y.; Yuan, Y. L1-Norm-Based 2DPCA. IEEE Trans. Syst. Man Cybern. Part B (Cybern.) 2010, 40, 1170–1175.
- 28. Wang, R.; Nie, F.; Yang, X.; Gao, F.; Yao, M. Robust 2DPCA With Non-greedy ℓ₁-Norm Maximization for Image Analysis. *IEEE Trans. Cybern.* **2015**, *45*, 1108–1112. [CrossRef] [PubMed]
- 29. Yang, X.; Wang, W.; Liu, L.; Shao, Y.; Zhang, L.; Deng, N. Robust 2DPCA by *Tℓ*₁ Criterion Maximization for Image Recognition. *IEEE Access* **2021**, *9*, 7690–7700. [CrossRef]
- 30. Wang, H.; Wang, J. 2DPCA with L1-norm for simultaneously robust and sparse modelling. *Neural Netw. Off. J. Int. Neural Netw. Soc.* 2013, 46, 190–198. [CrossRef]
- 31. Wang, J. Generalized 2-D Principal Component Analysis by Lp-Norm for Image Analysis. *IEEE Trans. Cybern.* **2016**, *46*, 792–803. [CrossRef]
- 32. Ding, C.; Zhou, D.; He, X.; Zha, H. R1-PCA: rotational invariant L1-norm principal component analysis for robust subspace factorization. In Proceedings of the 23rd International Conference on Machine Learning, Pittsburgh, PA, USA, 25–29 June 2006.
- 33. Nie, F.; Huang, H.; Cai, X.; Ding, C. Efficient and Robust Feature Selection via Joint L2, 1-Norms Minimization. In Proceedings of the NIPS, Vancouver, BC, Canada, 6–11 December 2010.
- 34. Gao, Q.; Xu, S.; Chen, F.; Ding, C.; Gao, X.; Li, Y. *R*₁-2-DPCA and Face Recognition. *IEEE Trans. Cybern.* **2019**, *49*, 1212–1223. [CrossRef]
- 35. Li, T.; Li, M.; Gao, Q.; Xie, D. F-norm distance metric based robust 2DPCA and face recognition. *Neural Netw. Off. J. Int. Neural Netw. Soc.* 2017, 94, 204–211. [CrossRef]
- 36. Gao, Q.; Ma, L.; Liu, Y.; Gao, X.; Nie, F. Angle 2DPCA: A New Formulation for 2DPCA. *IEEE Trans. Cybern.* **2018**, 48, 1672–1678. [CrossRef]
- 37. Wang, Y.; Li, Q. Robust 2DPCA With F-Norm Minimization. IEEE Access 2019, 7, 68083–68090. [CrossRef]
- 38. Wang, X.; Shi, L.; Liu, J.; Zhang, M. Cosine 2DPCA with Weighted Projection Maximization. *IEEE Trans. Neural Netw. Learn. Syst.* 2022, 1–14. [CrossRef] [PubMed]
- 39. Bi, P.; Deng, Y.; Du, X. A robust optimal mean cosine angle 2DPCA for image feature extraction. *Neural Comput. Appl.* **2022**, 34, 20117–20134. [CrossRef]
- 40. Razzak, I.; Abu-Saris, R.M.; Blumenstein, M.; Xu, G. Integrating joint feature selection into subspace learning: A formulation of 2DPCA for outliers robust feature selection. *Neural Netw. Off. J. Int. Neural Netw. Soc.* **2020**, *121*, 441–451. [CrossRef]
- 41. Mi, J.X.; Zhang, Y.N.; Li, Y.; Shu, Y. Generalized two-dimensional PCA based on L2, p-norm minimization. *Int. J. Mach. Learn. Cybern.* **2020**, *11*, 2421–2438. [CrossRef]
- 42. Zhou, G.; Xu, G.; Hao, J.; Chen, S.; Xu, J.; Zheng, X. Generalized Centered 2-D Principal Component Analysis. *IEEE Trans. Cybern.* **2021**, *51*, 1666–1677. [CrossRef]
- 43. Kuang, H.; Ye, W.; Zhu, Z. Research on Face Recognition Algorithm Based on Robust 2DPCA. *Adv. Pure Math.* **2021**, *11*, 149–161. [CrossRef]
- 44. Zhou, S.; Zhang, D. Bilateral Angle 2DPCA for Face Recognition. IEEE Signal Process. Lett. 2019, 26, 317–321. [CrossRef]
- 45. Bi, P.; Xu, J.; Du, X.; Li, J.; Chen, G. 12,p-norm sequential bilateral 2DPCA: A novel robust technology for underwater image classification and representation. *Neural Comput. Appl.* **2020**, *32*, 17027–17041. [CrossRef]
- 46. Xiang, X.; Yang, J.; Chen, Q. Color face recognition by PCA-like approach. Neurocomputing 2015, 152, 231–235. [CrossRef]
- 47. Jia, Z.; Ling, S.; Zhao, M. Color Two-Dimensional Principal Component Analysis for Face Recognition Based on Quaternion Model. In Proceedings of the ICIC, Liverpool, UK, 7–10 August 2017.
- 48. Xiao, X.; Zhou, Y. Two-Dimensional Quaternion PCA and Sparse PCA. *IEEE Trans. Neural Netw. Learn. Syst.* **2019**, *30*, 2028–2042. [CrossRef]
- 49. Wang, M.; Song, L.; Sun, K.; Jia, Z. F-2D-QPCA: A Quaternion Principal Component Analysis Method for Color Face Recognition. *IEEE Access* **2020**, *8*, 217437–217446. [CrossRef]
- 50. Jia, Z.; Qiu, Z.J.; Zhao, M. Generalized Two-Dimensional Quaternion Principal Component Analysis with Weighting for Color Image Recognition. *arXiv* **2020**, arXiv:2010.01477.

Appl. Sci. **2022**, 12, 12913 25 of 25

51. Zhao, M.; Jia, Z.; Cai, Y.; Chen, X.; Gong, D. Advanced variations of two-dimensional principal component analysis for face recognition. *Neurocomputing* **2021**, 452, 653–664. [CrossRef]

- 52. Zhang, F.; Yang, J.; Qian, J.; Xu, Y. Nuclear Norm-Based 2-DPCA for Extracting Features From Images. *IEEE Trans. Neural Netw. Learn. Syst.* **2015**, *26*, 2247–2260. [CrossRef]
- 53. Zhang, Z.; Zhou, S.; Li, D.; Yang, T. Riemannian proximal stochastic gradient descent for sparse 2DPCA. *Digit. Signal Process.* **2021**, *122*, 103320. [CrossRef]
- 54. Li, J.; Kang, Z.; Peng, C.; Chen, W. Self-Paced Two-dimensional PCA. In Proceedings of the AAAI, Virtual Event, 2–9 February 2021.
- 55. Wang, X.; Li, H.; Zhou, Y.; Zheng, H. Lanczos Algorithm for 2DPCA. J. Phys. Conf. Ser. 2021, 2025, 012035. [CrossRef]
- 56. Yu, D.; Wu, X. 2DPCANet: a deep leaning network for face recognition. Multimed. Tools Appl. 2018, 77, 12919–12934. [CrossRef]
- 57. Li, Y.; Wu, X.; Kittler, J. L1-2D2PCANet: A deep learning network for face recognition. *J. Electron. Imaging* **2018**, 28, 023016. [CrossRef]
- 58. Sykora, S. Mathematical Means and Averages: Basic Properties; Stan's Library: Castano Primo, Italy, 2009.
- 59. Lee, K.C.; Ho, J.; Kriegman, D.J. Acquiring linear subspaces for face recognition under variable lighting. *IEEE Trans. Pattern Anal. Mach. Intell.* **2005**, 27, 684–698.
- 60. Martinez, A.M. The AR Face Database; CVC Technical Report 24; Universitat Autònoma de Barcelona: Barcelona, Spain 1998.
- 61. Li, W.; Zhang, L.; Zhang, D.; Lu, G.; Yan, J. Efficient joint 2D and 3D palmprint matching with alignment refinement. In Proceedings of the IEEE Conference on Computer Vision and Pattern Recognition, San Francisco, CA, USA, 13–18 June 2010; pp. 795–801.
- 62. Hsu, C.W.; Chang, C.C.; Lin, C.J. A Practical Guide to Support Vector Classification. 2003. Available online: https://www.csie.ntu.edu.tw/~cjlin/papers/guide/guide.pdf (accessed on 18 November 2022).
- 63. Chang, C.C.; Lin, C.J. LIBSVM: A library for support vector machines. ACM Trans. Intell. Syst. Technol. 2011, 2, 27. [CrossRef]
- 64. Zhang, L.; Yang, M.; Feng, X. Sparse representation or collaborative representation: Which helps face recognition? In Proceedings of the IEEE International Conference on Computer Vision, Barcelona, Spain, 6–13 November 2011; pp. 471–478.
- 65. Zhang, L.; Yang, M.; Feng, X.; Ma, Y.; Zhang, D. Collaborative representation based classification for face recognition. arXiv 2012, arXiv:1204.2358.
- 66. Wang, J.; Zhang, B.; Xie, X.; Li, J.; Zhang, L.; Guo, H. Whole-brain Classification Based on Generalized Sparse Logistic Regression. *J. Xinyang Norm. Univ.* **2022**, *35*, 488–493.
- 67. Chihaoui, M.; Elkefi, A.; Bellil, W.; Amar, C.B. A Survey of 2D Face Recognition Techniques. Computers 2016, 5, 21. [CrossRef]
- 68. Naik, M.K.; Wunnava, A. Classical 2D Face Recognition: A Survey on Methods, Face Databases, and Performance Evaluation. In *Advances in Intelligent Computing and Communication, Proceedings of the ICAC 2019, Umea, Sweden, 16–20 June 2019*; Springer: Singapore, 2020; pp. 375–383.